

Photophysics of manisyl-substituted 2-pyridin-2-yl-1,10-phenanthrolines. Dual emission dependant on structure and solvent.

Jeremy K. Klosterman, Kim K. Baldridge and Jay S. Siegel*^a

^aOrganisch-chemisches Institut, Universität Zürich Winterthurerstrasse 190 Zürich, Switzerland CH-8057. E-mail:
jss@oci.uzh.ch

Supporting Information:

- Table S1** Absorption data for pyridyl-phenanthrolines **I α -I γ** .
Table S2 Absorption data for pyridyl-phenanthrolines **II(α - γ)**
Table S3 Absorption data for pyridyl-phenanthrolines **III α -III γ**
Figure S1 Solvent dependence of the absorption maxima for the first transition.
Figure S2 Dependence of fluorescence quantum yield on solvent polarity.
Figure S3 Excitation spectra of manisyl-substituted pyridyl-phenanthrolines [**I-III** × α - γ].
Figure S4 Representative experimental fluorescence decay curves of **II β** .
Figure S5 Representative fluorescence decay curve residuals of **II β** .
Figure S6 Mean fluorescence lifetimes vs solvent polarity $E_T(N)$ values.
Figure S7 Radiative rate constants k_f vs solvent polarity $E_T(N)$ values.
Figure S8 Calculated energies for the frontier orbitals of 1,10-phenanthroline, terpyridine, and 2-pyridin-2-yl-phenanthroline.
Figure S9 Unoccupied low-lying $a_2(\chi)$ and $b_1(y)$ orbitals of phenanthrolines.

Table S1 Absorption data for pyridyl-phenanthrolines I α -I γ .

	solvent	λ_{\max}	ε_{\max}	λ_{\max}	ε_{\max}
Iα	EtOH	293	32600	351	4300
	CH ₃ CN	293	31800	351	4000
	CH ₂ Cl ₂	294	32600	352	5100
	Et ₂ O	285	31800	352	4300
	CH	284	26000	352	4100
Iβ	EtOH	299	32400	353	7800
	CH ₃ CN	296	33300	354	7000
	CH ₂ Cl ₂	298	33200	354	8100
	Et ₂ O	295	35100	353	7500
	CH	296	31900	353	7700
Iγ	EtOH	287	16300	352	2300
	CH ₃ CN	291	14900	352	1900
	CH ₂ Cl ₂	286	19000	352	2800
	Et ₂ O	284	16200	351	2400
	CH	283	10900	351	2400

^a λ_{\max} in nm.

Table S3. Absorption data for pyridyl-phenanthrolines III α -III γ .

	solvent	λ_{\max}	ε_{\max}	λ_{\max}	ε_{\max}	λ_{\max}	ε_{\max}
IIIα	EtOH	289	36300	316	25600	352	4400
	CH ₃ CN	287	36700	314	26300	352	4700
	CH ₂ Cl ₂	288	33600	317	23700	352	4800
	Et ₂ O	287	35400	315	27600	353	4800
	CH	287	33700	315	26600	352	4900
IIIβ	EtOH	293	18100	316	15000	353	4900
	CH ₃ CN	291	29700	315	24900	353	4900
	CH ₂ Cl ₂	293	26400	319	22000	353	7500
	Et ₂ O	290	30900	315	27600	355	6900
	CH	290	22900	315	19000	353	7500
IIIγ	EtOH	291	36900	313	24400	354	5400
	CH ₃ CN	288	37900	312	24500	352	4500
	CH ₂ Cl ₂	290	36500	315	23800	352	4800
	Et ₂ O	288	38200	313	27200	353	5100
	CH	288	31100	313	23000	352	5100

^a λ_{\max} in nm.

Table S2 Absorption data for pyridyl-phenanthrolines II(α - γ).

	solvent	λ_{\max}	ε_{\max}	λ_{\max}	ε_{\max}	λ_{\max}	ε_{\max}
IIα	EtOH	295	31200	310	26160	353	4000
	CH ₃ CN	294	45800	310	36115	353	5300
	CH ₂ Cl ₂	295	39400	310	36115	354	5100
	Et ₂ O	294	44400	312	34778	353	5200
	CH	293	20300	312	16117	353	2500
IIβ	EtOH	298	37800	313	35663	354	8500
	CH ₃ CN	297	39200	311	36240	354	8500
	CH ₂ Cl ₂	298	42100	313	37573	355	9200
	Et ₂ O	295	44400	313	40389	354	8300
	CH	296	37700	313	33950	353	7800
IIγ	EtOH	295	38100	309	31005	353	4300
	CH ₃ CN	294	38600	308	29346	353	4000
	CH ₂ Cl ₂	295	38600	309	29846	353	4300
	Et ₂ O	293	39500	309	29765	352	4000
	CH	294	37500	309	28974	353	4000

^a λ_{\max} in nm.

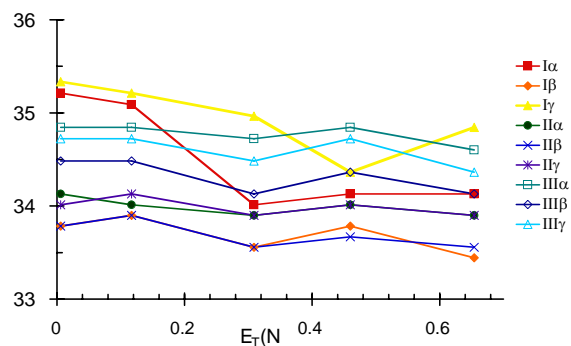


Figure S1. Solvent dependence of the absorption maxima for the first transition.

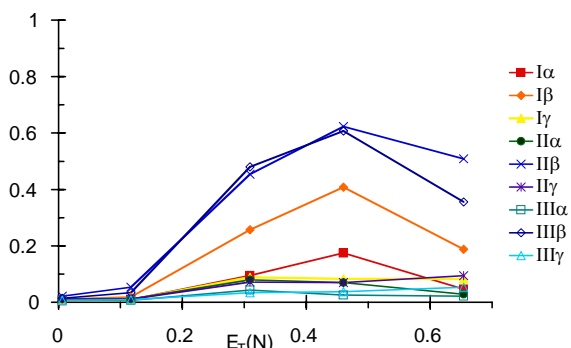


Figure S2. Dependence of fluorescence quantum yield on solvent polarity.

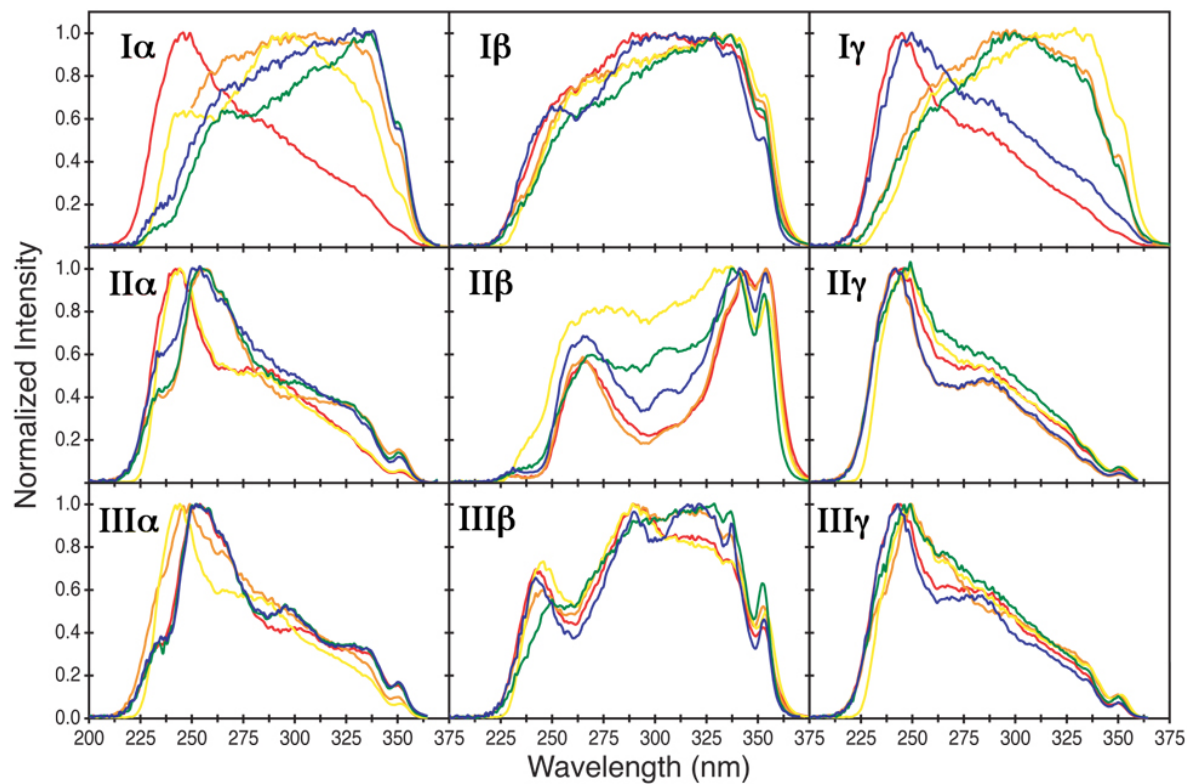


Figure S3. Excitation spectra of manisyl-substituted pyridyl-phenanthrolines [I–III \times α – γ] in ethanol (red), acetonitrile (orange), methylene chloride (yellow), diethyl ether (green), and cyclohexane (blue) at room temperature.

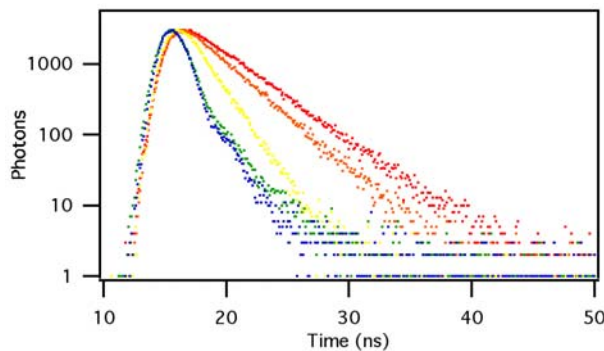


Figure S4 Representative experimental fluorescence decay curves of $\text{II}\beta$ in ethanol (red), acetonitrile (orange), methylene chloride (yellow), diethyl ether (green), and cyclohexane (blue) at room temperature.

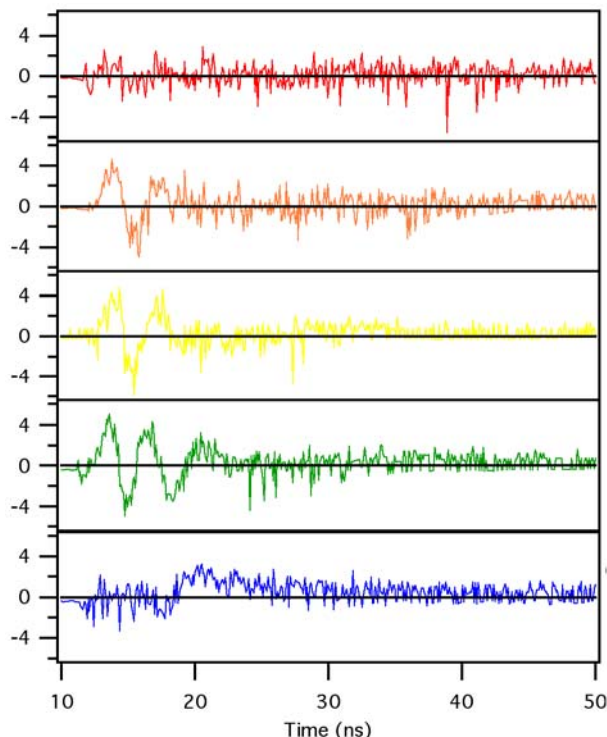


Figure S5 Representative fluorescence decay curve residuals of $\text{II}\beta$ in ethanol (red), acetonitrile (orange), methylene chloride (yellow), diethyl ether (green), and cyclohexane (blue) at room temperature.

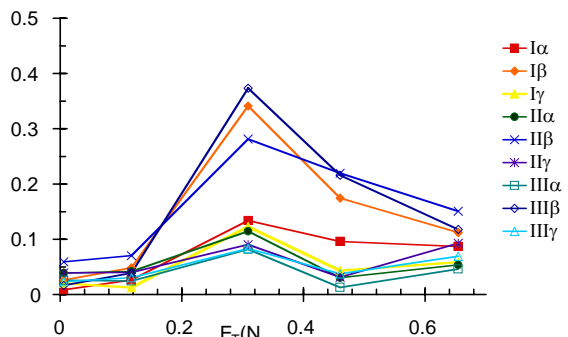


Figure S7 Radiative rate constants k_f vs solvent polarity $E_{\text{T}}(\text{N})$ values.

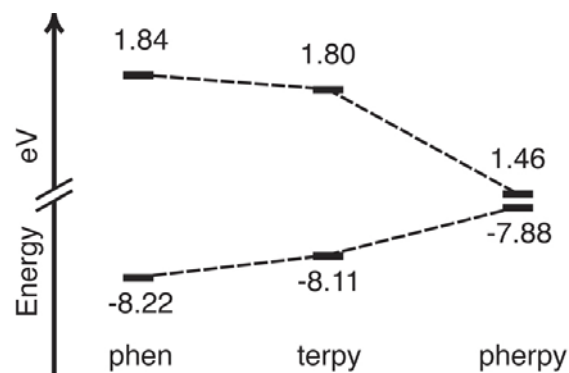


Figure S8. Calculated energies for the frontier orbitals of 1,10-phenanthroline (phen) **A**, terpyridine (terpy) **B**, and 2-pyridin-2-yl-phenanthroline (pherry) **C**. The LUMO orbitals have positive energies while the energies are negative for the HOMO orbitals

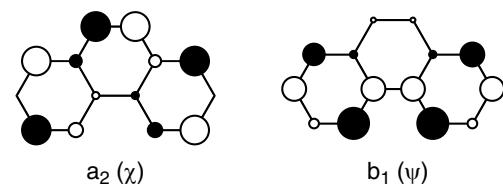


Figure S9 Unoccupied low-lying $a_2(\chi)$ and $b_1(\psi)$ orbitals of phenanthrolines.

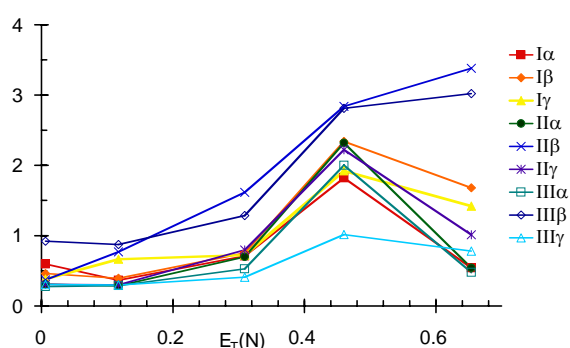


Figure S6 Mean fluorescence lifetimes vs solvent polarity $E_{\text{T}}(\text{N})$ values.